



Thermally activated reconstruction of $\text{TiO}_2(1\ 1\ 0)-(1 \times 1)$ surface in the presence of potassium: An STM study

Z. Majzik^{a,1}, N. Balázs^b, A. Berkó^{b,*}

^a Department of Physical Chemistry and Material Science, Faculty of Science and Informatics, University of Szeged, H-6720 Szeged, Aradi Vértanúk tere 1, Hungary

^b Reaction Kinetics Laboratory, Institute of Nanochemistry and Catalysis, Chemical Research Center of the Hungarian Academy of Sciences, H-1025 Budapest, Pusztaszeri út 59-67, Hungary

ARTICLE INFO

Article history:

Received 30 March 2011

Received in revised form 13 May 2011

Accepted 21 June 2011

Available online 26 July 2011

Keywords:

$\text{TiO}_2(1\ 1\ 0)$

K

STM-AES-TPD

2D model catalyst

Alkali promoters

ABSTRACT

The deposition of potassium onto $\text{TiO}_2(1\ 1\ 0)$ surface at 330 K and the effects of post-annealing are investigated by scanning tunneling microscopy (STM), thermal desorption spectroscopy (TDS) and Auger-electron spectroscopy (AES). At lower K coverages (a few percentage of a monolayer), 3–4 nm long and 1–2 nm wide islands appear which can be identified with K covered regions. At higher K coverages, the surface exhibits disordered structures. Depending on the initial K coverage, the annealing above 700 K in UHV results in ordering of the surface. For app. 1/3 monolayer K and annealing at around 900 K, the entire surface reconstructs into a (1×2) phase accompanied by the appearance of pits with an average diameter of 20–30 nm. This morphology is characteristic up to 1000 K. Above this temperature, the recovery of the (1×1) phase was observed. At low K coverages (<0.2 ML) the annealing at 1000 K resulted in the formation of protruding islands of approximately $2 \times 2\ \text{nm}^2$ which were identified with a strongly bonded surface compound containing K.

© 2011 Elsevier B.V. All rights reserved.

1. Introduction

Alkali metal compounds are extensively applied as promoter additives for the preparation of catalysts and gas sensors [1–3]. During the last decades, most of the studies in connection of the effects of alkali metals have been focused on metal and semiconductor surfaces [4–6]. Much less attention has been given to the interaction between alkali metals and oxide surfaces, although this type of experimental and theoretical works are very important for elucidating some important issues in the fine tuning of catalytic performance. By the application of two-dimensional metal-oxide model systems (planar catalysts), the complex effects of the additives can be efficiently studied [7]. The effect of the different additives can substantially be two-fold: an electronic and/or a morphological one. These two phenomena are often difficult to separate, since there is usually a strong interplay between them.

In a recent work, we studied the influence of the pre-adsorbed potassium on the nanoscale morphology of Au deposited on a

$\text{TiO}_2(1\ 1\ 0)$ surface [8]. It was found that the surface K sensitively affects the particle formation of gold. At room temperature, gold exhibits higher dispersity in the presence of K, however, at above 500–600 K, especially for higher K coverages (1–2 monolayer ML), a very intensive aggregation of the gold particles takes place. Since the finding of the high activity of supported Au-catalysts in the low temperature oxidation of CO, a tremendous work has been done for the understanding of this reaction in detail and for the development of more efficient gold catalysts [9–11]. Potassium belongs to the so called reactive admetals on reducible oxide substrates, like TiO_2 , where the formation of a strong K–O bond and the reduction of the support were deduced from sophisticated photoelectron spectroscopy measurements, like ARUPS, and SEX-AFS [12–18]. Although a complete charge transfer was assumed between K(2s) and Ti(4d) orbitals resulting in the reduction of Ti^{4+} to Ti^{3+} , a clear experimental detection of this latter species failed. This phenomenon was explained by the delocalization of transferred charge among the adjacent Ti ions [16]. The screening of surface phonon modes detected by HREELS also supports the idea that potassium forms oxide species at room temperature at K coverages above 1 ML [15]. These experimental observations were studied and explained also by theoretical calculations [16,19–21]. The importance of the subsurface oxidation state was also shown for K/ TiO_2 system by proving that the formation of detectable amount of Ti^{3+} species in XPS spectra sensitively varies for stoichiometric and non-stoichiometric (bulk state) samples [17]. Thermal

* Corresponding author at: P.O. Box 168, H-6701 Szeged, Hungary.

Tel.: +36 62 544 646; fax: +36 62 420 678.

E-mail address: aberko@chem.u-szeged.hu (A. Berkó).

¹ Present address: Department of Thin Films, Institute of Physics of the Academy of Sciences of Czech Republic, Cukrovarnicka 10, Prague 6, 162 53 Czech Republic.

desorption of K and Cs on $\text{TiO}_2(110)$ surface was also investigated in detail [22,23]. Moreover, atomic scale studies by STM and AFM methods were also performed in several cases for alkali metal atoms adsorbed on $\text{TiO}_2(110)$ surfaces [8,18]. In harmony with the earlier SEXAFS measurements and theoretical calculations, the main conclusion of these studies is that K adsorbs preferentially in three-fold hollow sites formed by two bridging and one in-plane oxygen atoms of the substrate. Furthermore, the increase of the coverage results in a decrease of the bonding energy between potassium and the substrate, as a consequence of the repulsive interaction between the K ions. At the same time, this interaction cannot prevent the formation of K-covered islands, especially at lower coverages. All of these results strongly suggest that the electronic and morphological effects combine strongly and it should be taken into account in the interpretation of any special phenomenon related to alkali additives.

In the present work, the effect of coverage and annealing temperature on the morphology of K deposited $\text{TiO}_2(110)$ surface are studied mainly by scanning tunneling microscopy (STM). In addition, some thermal desorption spectroscopy (TDS) and Auger-electron spectroscopy (AES) results are also presented.

2. Experimental

The experiments were carried out in an UHV chamber equipped with a room temperature scanning tunneling microscope (WA-Technology), a cylindrical mirror analyzer for Auger-electron spectroscopy (AES) and a quadrupole mass spectrometer for gas phase analysis (TDS).

$\text{TiO}_2(110)$ single crystals were directly fixed to a Ta filament by oxide adhesive (ceramobond 571, AREMCO Products) and mounted on a transferable sample holder. The probe was ohmically heated by the current flowing through the Ta filament. The temperature was measured by a chromel–alumel (K-type) thermocouple stuck to the side of the sample. An initial cleaning procedure consisted of a slow (0.1 K s^{-1}) increase of the temperature up to 1050 K and of several hours of Ar^+ bombardment at ion energy of 1–2 keV and ion current density of $5 \mu\text{A cm}^{-2}$. This procedure resulted in not only the purification of the sample (mainly from Ca and K contamination) but caused also some reduction in the subsurface layers, thus made it possible to avoid charging problems during the spectroscopy and microscopy measurements. From time to time (after an extended use of the sample) the surface was reoxidized in 5×10^{-4} mbar oxygen for 15 min at 900 K. The final treatment was usually a short annealing at 1050 K in UHV. The heating rate never exceeded the value of 2 K s^{-1} . The surface of the $\text{TiO}_2(110)$ probe obtained in this way exhibited mainly (1×1) ordered phase accompanied by some (3–5% of the total surface area) protruding dots and 1D stripes in the $[001]$ orientation [24].

The cleanliness of the sample and the deposited metal layer were checked by Auger-electron spectroscopy (AES). The surface morphology was monitored by scanning tunneling microscopy (STM). Commercial getter sources (SAES) were used for K-deposition. The K coverage is expressed in monolayer equivalent (ML), which corresponds to app. 5.2×10^{14} K atom/ cm^2 by assuming that each unit cell of the support lattice contains a single K atom [8,18]. It should be remarked, however, that the definition and the determination of K concentration is rather controversial in the literature. For example Heise and Courth associated 2 K atoms per unit cell with 1 ML of K (10.4×10^{14} K atom/ cm^2) [14]. Nevertheless, by taking into account the previous estimations for the K coverage and considering the potassium surface atom density (6.6×10^{14} K atom/ cm^2), the first definition for 1 ML (5.2×10^{14} K atom/ cm^2) seems to be the most appropriate value for our experiments where K was deposited at around 330 K.

For STM imaging, chemically edged W-tips were applied and sharpened “in situ” over the TiO_2 surface by using 5–10 V pulses. Typical tunneling parameter of +3 V (0.1 nA) was applied due to the relatively high band gap of the overlayer. In the case of clean surface, the imaging bias of +1.5 V proved to be sufficient.

3. Results

3.1. AES and STM detection of K adsorption on $\text{TiO}_2(110)$

Potassium was deposited on a clean $\text{TiO}_2(110)-(1 \times 1)$ surface exhibiting bulk terminated atomic positions (see STM imaging below) and Auger peaks characteristic of Ti and O. During the deposition, the temperature was kept slightly above room temperature (330 K). The potassium deposition was followed by measuring the peak-to-peak values of K(LMM) at 252 eV and Ti(LMM) at 385 eV on AES curves (dN/dE) and by determining their relative intensities (R_K) (Fig. 1A). It can be seen that in the function of the duration, R_K increases almost linearly up to 1 and asymptotically reaches a saturation value of app. 2.80 after 120 s deposition. This curve-shape depends naturally on the heating current used for the K-source and this duration-dependence was fixed during this work by tuning the heating current from time to time. As it was mentioned above, the saturation amount of deposited potassium at 330 K can be assigned to the concentration of the unit cells on a $\text{TiO}_2(110)$ surface (5.2×10^{14} K atom/ cm^2), accordingly, the value of R_K (~ 2.8) corresponds to one monolayer coverage ($\Theta_K = 1 \text{ ML}$). It can be assumed that the peak-to-peak Auger-signal intensity is proportional to the surface concentration of K (at least up to one monolayer) in a good approximation, however, the relative intensities (R_K), mainly because of the shadowing effect, correlate only roughly with the surface concentration of potassium. Naturally, to measure the absolute intensity is experimentally much more difficult than to determine the relative intensities. By taking into account that due to the shadowing effect of the K overlayer, the decrease of the absolute intensity of the Ti signal is ca. 25–30%, the error of the coverage calcu-

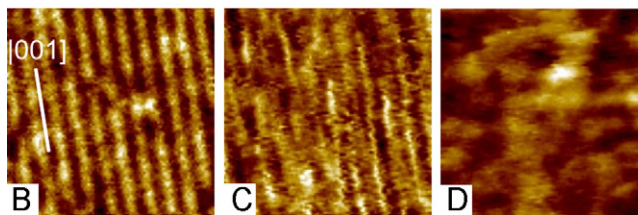
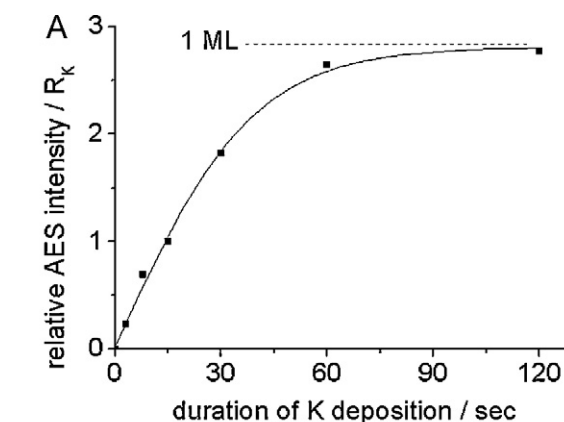


Fig. 1. (A) Change of the relative AES intensity ($R_K = I_{K-252 \text{ eV}}/I_{Ti-385 \text{ eV}}$) as a function of the duration of K deposition at 330 K. Characteristic STM images of $7 \times 7 \text{ nm}^2$ recorded on (B) clean $\text{TiO}_2(110)-(1 \times 1)$ and covered by (C) 0.09 ML, (D) 0.55 ML of potassium.

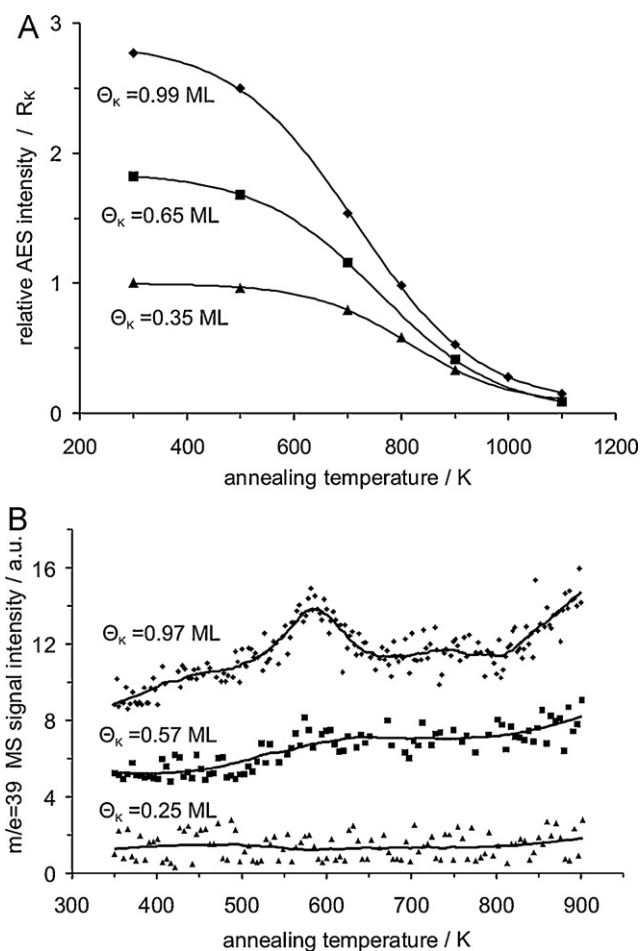


Fig. 2. (A) Change of the relative AES intensity (R_K) as a function of the annealing temperature for three initial K coverages; (B) thermal desorption curves (TDS) of K recorded at $m/e = 39$ for different initial K coverages (heating rate is 2 K s^{-1}).

lation is max 20–30% in our case, when we use R_K as a linear indicator for the coverage: 1 ML ($5.2 \times 10^{14} \text{ K atom/cm}^2$) belongs to $R_K = 2.80$.

The saturation of the potassium adlayer was followed also by recording STM images. Fig. 1 shows the characteristic images of clean (B) and K covered surfaces of 0.09 ML (C) and 0.55 ML (D). The clean surface exhibits dark and bright lines running in parallel with a distance of 6.5 nm. This morphology is characteristic for (1×1) bulk terminated arrangement where the bright rows can be identified with five-fold coordinated Ti^{4+} sites (Fig. 1B). At $\Theta_K = 0.09 \text{ ML}$, elongated dark islands appear at the place of the bright rows (Fig. 1C). This behaviour is in harmony with the earlier observations presented for low K-coverage [18]. In the case of 0.55 ML coverage the dark pits and white dots constitute a rather unordered surface structure (Fig. 1D), although larger scale images (not shown here) indicate some ordering in the $[001]$ direction. For even higher K-coverages, the surface exhibited only strongly disordered structures.

3.2. Annealing of K/TiO₂(1 1 0) surfaces: AES and TDS measurements

In this series of experiments, TiO₂(1 1 0) surfaces were initially deposited by different amount of potassium at near room temperature (330 K) and were subsequently annealed for 2 min at elevated temperatures between 300 K and 1100 K. Auger-electron

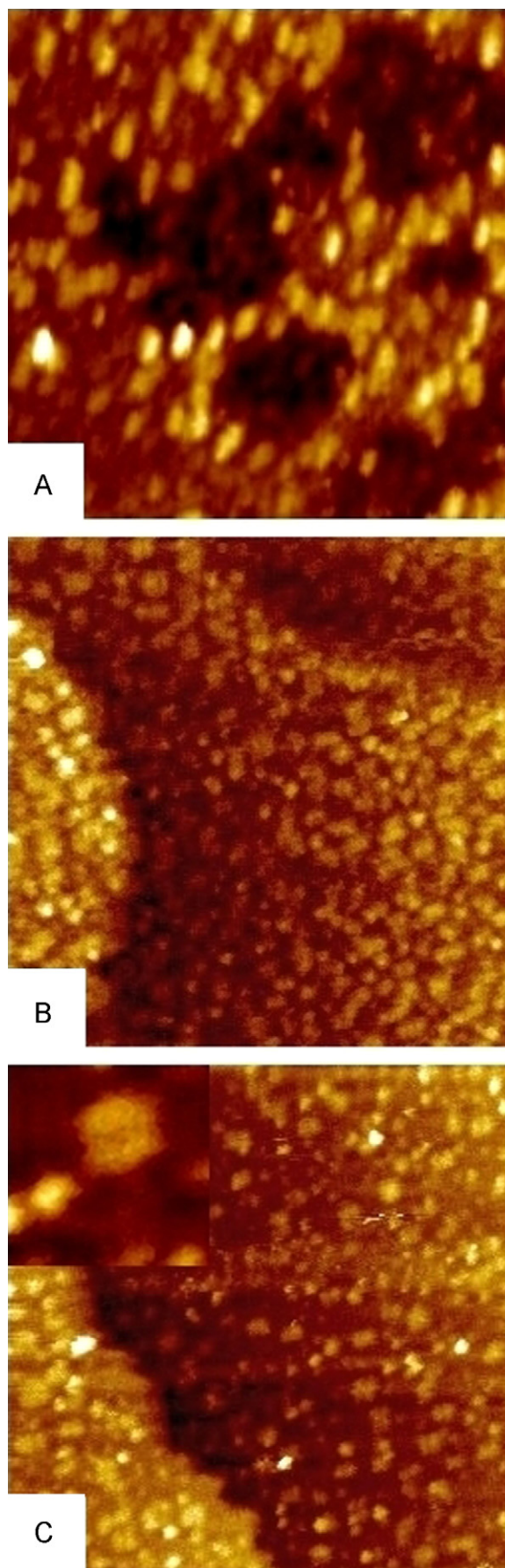


Fig. 3. STM images ($50 \times 50 \text{ nm}^2$) recorded on K deposited (0.09 ML) TiO₂(1 1 0) surface annealed at (A) 900 K, (B) 1000 K and (C) 1100 K for 2 min.

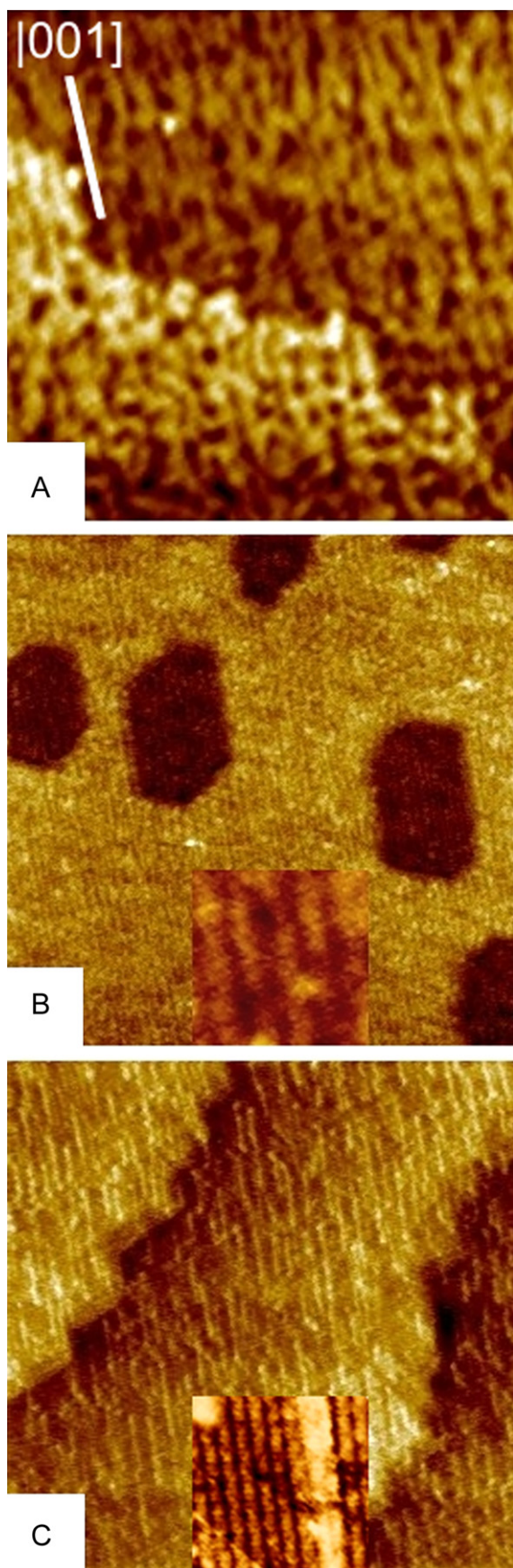


Fig. 4. STM images ($100 \times 100 \text{ nm}^2$) recorded on $\text{TiO}_2(110)-(1 \times 1)$ surface deposited by K of 0.36 ML at 330 K and annealed at (A) 700 K, (B) 900 K and (D) 1100 K for 2 min. The size of the STM images inserted in B and C (bottom middle) is $7 \times 7 \text{ nm}^2$.

spectroscopy measurements plotted in Fig. 2A were performed for three initial K coverages: $\Theta_{\text{K}} = 0.35 \text{ ML}$ ($R_{\text{K}} = 1.00$), $\Theta_{\text{K}} = 0.65 \text{ ML}$ ($R_{\text{K}} = 1.82$) and 0.99 ML ($R_{\text{K}} = 2.77$). The change of the relative AES intensities indicates that after a slight decrease between 300 K and 500 K, a significant and gradual loss of the K signal can be detected between 500 K and 900 K for each probe. The curves show that the higher the coverage the lower the temperature where the maximum rate of the potassium loss appears. For example, in the case of the lowest initial coverage ($R_{\text{K}} = 0.35$), the decrease of the K signal begins only above 700 K. It can also be seen that all the three curves approach a similar value ($\sim R_{\text{K}} = 0.10$) in the range between 900 K and 1100 K. This means that it is impossible to entirely clean the surface from K by a few minutes annealing at 1100 K. It is worth remarking that to remove all potassium, the surface had to be bombarded by Ar^+ ions and annealed for a few minutes at 1100 K.

The thermal desorption curves recorded for $m/e = 39$ mass spectrometer (MS) signal (characteristic of atomic K) after the deposition of different amount of K at near room temperature (330 K) are presented in Fig. 2B. The heating rate of 2 K s^{-1} was applied in each case. The temperature range of the plots is limited to 900 K because the MS signal increases very intensively (especially for higher K coverages) above this temperature. We assume that this behaviour is due to the desorption from the sample holder or to the appearance of K ions among the desorbing species. For 0.25 ML (or less), the MS signal of $m/e = 39$ shows a very small feature at around 450 K and above 800 K. More pronounced desorption traces appear for $\Theta_{\text{K}} = 0.57 \text{ ML}$ and $\Theta_{\text{K}} = 0.97 \text{ ML}$ initial coverages. These latter curves are peaked at around 550 K and 900 K and smaller desorption features appear at 400 K and 750 K. The wide temperature range is a typical feature of alkali metal desorption from different metal and oxide surfaces and can be explained by a gradual decrease of the activation energy (bonding energy) with the coverage. It is worth to note that the region around 550 K for the initial K coverage higher than 0.5–0.6 ML can be ascribed to simultaneous desorption of CO_2 and K due to decomposition of some surface K_2CO_3 contamination. Some C contamination of the K adlayer was also detectable in the range of 0.5–1.0 ML by Auger-spectroscopy. We have looked for other desorption species like KO, K_2O , KO_2 , O_2 and K_2TiO_3 . It was found that a weak intensity KO desorption can be detected in the temperature range of 800–900 K for higher K coverages.

3.3. Annealing of $\text{K}/\text{TiO}_2(110)$ surfaces: morphological characterization by STM

As mentioned above, in the case of low K coverages ($\Theta_{\text{K}} < 0.2 \text{ ML}$), annealing up to 900 K causes only a moderate change in the relative AES signal intensity of K. In contrast to this stability, STM images indicate substantial morphological changes of the atomic terraces: the terrace edges became lacy and small dots of 1–2 nm appear on $\text{TiO}_2(110)-(1 \times 1)$ surface exposed to 0.09 ML potassium at 330 K and annealed at 900 K for 2 min (Fig. 3A). Further annealing at 1000 K for 2 min results in straight line edges, at the same time the terraces are covered with quasi rectangular or slightly elongated clusters (Fig. 3B). The concentration of latter species decreases on the effect of annealing at 1100 K for 2 min (Fig. 3C). Supposing that these clusters can be identified with nanoparticles containing K, their disappearance is in good harmony with the gradual decrease of R_{K} (see Fig. 2A) in this temperature range. From this fact it can be concluded that these nanoclusters consist of some surface K compound, which – instead of agglomeration into larger crystallites – disappears (desorb from the surface or diffuse into the bulk) in a relatively slow process. The insert of $7 \times 7 \text{ nm}^2$ in Fig. 3C (top left) exhibits a typical island with a height of 0.2 nm.

A similar deposition/annealing experiment was also performed for a K coverage of 0.36 ML (Fig. 4). The surface structures obtained after different K depositions at near room temperature have already been presented above (Fig. 1). The STM image of $50 \times 50 \text{ nm}^2$ in Fig. 4A shows a characteristic surface morphology appearing after a thermal treatment at 700 K in UHV for 2 min. Some ordering of the surface in the $[001]$ direction can obviously be seen, nevertheless, the general morphology of the surface refers to some “etching” process. The average periodicity of the deep and the protruding rows is approximately $5 (\pm 0.5) \text{ nm}$ and the variation of the height is 0.3–0.4 nm. Further annealing at 900 K results in agglomeration of the islands without any significant change of the average surface corrugation of 0.5 nm (the Z-distance between the lowest and the highest point of the image) (Fig. 4B). It should be remarked that in accordance with the AES measurements presented in Fig. 2A, this is the temperature regime where the largest K loss appears. This treatment results in the appearance of a completely new ordering: 1 atomic layer deep leaky terraces and almost fully periodic arrangement of $[001]$ direction on the atomic terraces decorated by some outrising nanodots. The lateral distance between the rows is 1.3 nm measured on the $7 \times 7 \text{ nm}^2$ image which corresponds unambiguously to a (1×2) reconstruction (bottom middle insert in Fig. 4B). This structure is well known from earlier studies and it was identified with the protruding Ti_2O_3 stripes running parallel to the $[001]$ direction [7]. The fact that the surface is almost completely transformed into (1×2) reconstruction, suggests a stoichiometric removal of oxygen of approximately 0.5 ML (one oxygen atom from every second unit cell of the support: $2\text{TiO}_2 = \text{Ti}_2\text{O}_3 + \text{O}$) from the entire surface layer. The other surprising result is that one atomic deep terrace pits are formed in 20–30% of the layer. This latter feature can tentatively be explained also by the removal of Ti from the surface layer what suggests a desorption of both K–O and K–Ti–O compounds. Note that only at this K coverage ($\sim 1/3 \text{ ML}$) was it possible to obtain an almost completely (1×2) reconstructed surface. Further annealing (2 min) at 1100 K resulted in a $(1 \times 2) \rightarrow (1 \times 1)$ phase transition (Fig. 4C). The lateral distance between the rows is 0.65 nm measured on the $7 \times 7 \text{ nm}^2$ image inserted in Fig. 4C (bottom middle). Note, that the bulk terminated (1×1) surface thus obtained shows higher concentration of reduced 1D stripes (presumably having a Ti_2O_3 composition) than that for the initial surface (before the deposition of K at near room temperature). This change in the surface morphology can easily be explained with the oxidation of the reduced top layer by the subsurface oxygen segregating to the surface.

The effect of the variation of the initial K coverage can be seen on the images presented in Fig. 5. The disturbed atomic terraces formed after annealing at 900 K can be compared. In the case of a low K coverage (0.09 ML), the surface exhibits the formation of flat terraces decorated by small nanoparticles described above (Figs. 5A and 3). At approximately $1/3 \text{ ML}$ coverage, the same treatment results in the formation of pits and a reconstruction into

(1×2) arrangement (Fig. 5B). By further increasing the initial K coverage, the extension of the pits becomes sufficiently large for the appearance of protruding islands (Fig. 5C). The different terrace composition developed suggests that the removal (“etching”) of the upper plane of the support is certainly connected to the initial K concentration.

4. Discussion

In the former electron and photoelectron spectroscopy studies, it was clearly shown that K atom adsorbs on oxygen sites through forming ionic bond [16,18]. Some works argued for the formation of KO surface compound, although the spectral features of this species cannot be identified with bulk potassium-oxides [15]. It was calculated that the charge of K(4s) orbital is transferred to the Ti(3d) level through the bond formed between oxygen and K, however, this process is probably not localized only on a single neighbouring Ti ion but spreads out to several surface and subsurface Ti ions [16,18]. By this assumption, it was possible to explain the absence of an intensive Ti^{3+} XPS signal. Pang et al. have shown that the STM images recorded on a $\text{TiO}_2(110)$ surface deposited by 0.03 ML of K at room temperature suggest a formation of $[001]$ oriented alternate-row islands of K atoms [18]. In our case, the appearance of elongated dark regions along the $[001]$ orientation can also be assigned to this structure (Fig. 1C, $\Theta_{\text{K}} = 0.09 \text{ ML}$). At the same time, by further increasing the K coverage, our STM images indicated the presence of disordered phases. The appearance of a disordered surface structure suggests that different chemical reactions proceed at the K– TiO_2 interface at around room temperature. On the effect of the adsorption of K atoms, the bond strength between an O ion and a Ti ion decreases by the formation of more reduced Ti ions. It means also that the oxygen ions located around the adsorbed K atoms become more reactive. We may assume that ordering of the K atoms into islands at very low K coverages is governed by this process. By increasing the surface concentration of K, it can be assumed that a given portion of K atoms have the ability to form more localized bond with the surface oxygen resulting in K_xO or K_xTiO_y (potassium metatitanate) toplayer complexes. These latter reactions (probably exothermic ones) can contribute to a dramatic restructuring of the upper atomic layers and can cause a disordering of the surface already at near room temperature.

According to our best knowledge, this is the first systematic STM study on the thermal behaviour of a K-deposited TiO_2 single crystal surface. The thermally induced morphological changes studied for lower K coverage (app. 0.1 ML) clearly indicate that in spite of the very slight change of the relative K Auger-signal and the lack of desorbing species detectable by TPD measurements, the STM indicates a huge material transport in the surface layers even below 900 K (Figs. 2 and 3). The splitting of terraces is especially an interesting

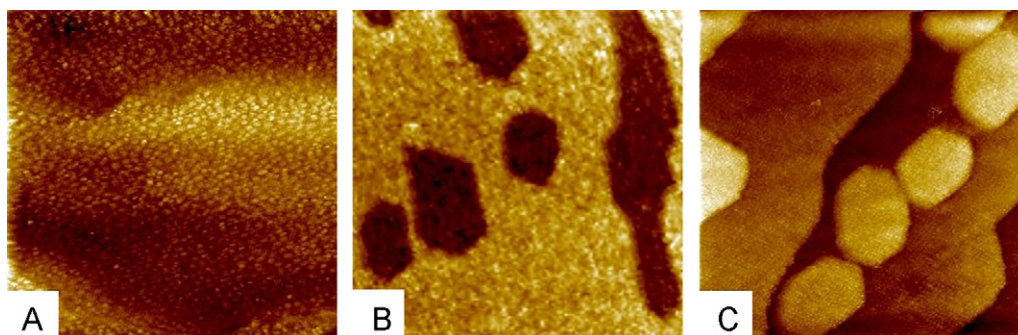


Fig. 5. STM images ($100 \times 100 \text{ nm}^2$) taken up after different K depositions at 330 K and annealing at 900 K for 2 min: (A) 0.09 ML, (B) 0.35 ML and (C) 0.66 ML.

feature suggesting that Ti ions become also mobile in the presence of surface K at this low concentration. Above 900 K, the nanocrystallites distributed on the reordered (1×1) terraces can be ascribed to strongly bonded K–O or K–Ti–O phases. Taking into account the low intensity of the AES signal and the relatively large coverage of islands found by STM (Fig. 3B), it can be assumed that the K atom is immersed in the interface (subsurface) layer [25]. For larger K coverages ($\sim 1/3$ ML) we have found even more dramatic rearrangements in the surface layers (Fig. 4). The disordered surface at room temperature exhibits a gradual ordering on the effect of increasing the temperature and at 900 K a complete (1×2) reconstruction takes place. This result contradicts somehow to LEED patterns obtained earlier by Hayden and Nicholson where a $\text{TiO}_2(1\ 1\ 0)$ surface covered by 3 ML of K at 140 K and heated up to 700 K exhibited a $c(2 \times 2)$ ordered phase [22]. These authors associated this phase to the formation of a strongly bonded potassium monolayer which is not really reasonable in the light of the present study. Although the presence of K is evidenced by AES measurements for the (1×2) reconstructed surface (Figs. 2A and 4B), the contribution of this element to the structure is probably negligible. Accordingly, we have to assume that this phase consists of Ti_2O_3 stripes running in parallel with the [001] orientation and this structure is the well known (1×2) reconstructed phase of the $\text{TiO}_2(1\ 1\ 0)$ surface. In other words, the TiO_2 surface is completely reduced on the effect of annealing in the presence of surface potassium. This feature is quite similar to that described for the Cs/ $\text{TiO}_2(1\ 1\ 0)$ system [23]. In this work, it was assumed that the partial reduction of TiO_2 by adsorbed K or Cs and the formation of a mixed alkali-metal–Ti oxide may be thermodynamically preferred. From experimental aspects, a weak point of this argument could be that, in our case, no other desorbed species, but potassium and a very low intensity KO signal, were detected. In an earlier paper, the bulk to surface diffusion of Ti ions was studied and it was concluded that below 900 K the segregation of Ti to the surface is strongly retarded [26]. In this way, only the pits appeared on the $\text{TiO}_2(1\ 1\ 0)$ atomic terraces (Fig. 4B) suggest that a compound containing Ti was also desorbed.

5. Conclusion

At very low coverages (<0.05 ML), the potassium deposited on a bulk terminated $\text{TiO}_2(1\ 1\ 0)$ –(1×1) surface at room temperature forms 1D-like islands in harmony with the previous observations, however, at higher K coverages (up to 1 ML), only disordered structures were detected by scanning tunneling microscopy. The annealing of the K covered $\text{TiO}_2(1\ 1\ 0)$ surfaces caused a gradual decrease of the amount of potassium in the range of 400 and 1000 K, as it was shown by AES and TDS measurements. The strong interaction of the surface potassium with the support oxide showed itself in a complete reordering of the terrace structure and the splitting of the terraces (etching-like behaviour) as an effect of the annealing at elevated temperatures. Moreover, at around $1/3$ ML potassium coverage, the thermal treatment at 900 K resulted in a complete reordering of the bulk terminated surface

into a (1×2) reconstructed arrangement indicating that the oxide surface became strongly reduced. The appearance of pits in the terraces detected by STM imaging, suggests the formation and the desorption of some Ti–K–O surface compound, although, we could not detect any species of this type by thermal desorption mass spectrometry. The annealing at even higher (1050 K) temperatures resulted in the reappearance of the (1×1) registry of the $\text{TiO}_2(1\ 1\ 0)$ surface (re-oxidation of the support surface). This latter process may be connected to the segregation of oxygen from the subsurface region. Furthermore, nanocrystalline 2D species of approximately 2 nm lateral extension containing K and Ti atoms were observed by STM for 0.10–0.15 ML K initial coverages at room temperature followed by annealing at 950–1050 K.

Acknowledgements

The authors gratefully thank the pleasant and fruitful discussions with Dr. László Óvári. This work was supported by the Hungarian Scientific Research Fund (OTKA) through K69200 and K81660 projects.

References

- [1] M.P. Kiskinova, *Poisoning and Promotion in Catalysis Based on Surface Science Concepts and Experiments*, Elsevier, Amsterdam, 1992.
- [2] H.J. Freund, M.W. Roberts, *Surf. Sci. Rep.* 25 (1996) 225.
- [3] G. Gusmano, A. Bianco, G. Montesperelli, E. Traversa, *Electrochim. Acta* 41 (7–8) (1996) 1359.
- [4] H.P. Bonzel, G. Pirug, in: D.A. King, D.P. Woodruff (Eds.), *Chemical Physics of Solid Surfaces*, vol. 6, Coadsorption, Promoters and Poisons, Elsevier, Amsterdam, 1993.
- [5] G. Ertl, in: H.P. Bonzel, A.M. Bradshaw, G. Ertl (Eds.), *The Physics and Chemistry of AM Adsorption*, Elsevier, Amsterdam, 1989.
- [6] F. Bechstedt, M. Scheffler, *Surf. Sci. Rep.* 18 (1993) 145.
- [7] U. Diebold, *Surf. Sci. Rep.* 48 (2003) 53.
- [8] A.M. Kiss, M. Švec, A. Berkó, *Surf. Sci.* 600 (2006) 3352.
- [9] M. Haruta, *Catal. Today* 36 (1997) 153.
- [10] M.M. Schubert, S. Hackenberg, A.C. van Veen, M. Muhler, V. Plzak, R.J. Behm, *J. Catal.* 197 (2001) 113.
- [11] M.S. Chen, D.W. Goodman, *Science* 306 (2004) 252.
- [12] P.J. Hardman, R. Casanova, K. Prabhakaran, C.A. Muryn, P.L. Wincott, G. Thornton, *Surf. Sci.* 269/270 (1992) 677.
- [13] K. Prabhakaran, D. Purdie, R. Casanova, C.A. Muryn, P.J. Hardman, P.L. Wincott, G. Thornton, *Phys. Rev. B* 45 (12) (1992) 6969.
- [14] R. Heise, R. Courths, *Surf. Sci.* 331–333 (1995) 1460.
- [15] A.G. Thomas, P.J. Hardman, C.A. Muryn, H.S. Dhariwal, A.F. Prime, G. Thornton, E. Román, J.L. de Segovia, *J. Chem. Soc. Faraday Trans.* 91 (20) (1995) 3569.
- [16] R. Lindsay, E. Michelangeli, B.G. Daniels, M.N. Polcik, A. Verdini, L. Floreano, A. Morgante, J. Muscat, N.M. Harrison, G. Thornton, *Surf. Sci.* 547 (2003) L859.
- [17] R. Lindsay, E. Michelangeli, B.G. Daniels, M. Polcik, A. Verdini, L. Floreano, A. Morgante, G. Thornton, *Surf. Sci.* 566 (2004) 921.
- [18] C.L. Pang, C.A. Muryn, A.P. Woodhead, H. Raza, S.S. Haycock, V.R. Dhanak, G. Thornton, *Surf. Sci.* 583 (2005) L147.
- [19] S. Krischok, J. Günster, W.D. Goodman, O. Höfft, V. Kemper, *Surf. Interface Anal.* 36 (2004) 77.
- [20] J. Muscat, N.M. Harrison, G. Thornton, *Phys. Rev. B* 59 (23) (1999) 15457.
- [21] T. Bredow, E. Aprà, M. Catti, G. Pacchioni, *Surf. Sci.* 418 (1998) 150.
- [22] B.E. Hayden, G.P. Nicholson, *Surf. Sci.* 274 (1992) 277.
- [23] A.W. Grant, C.T. Campbell, *Phys. Rev. B* 55 (3) (1997) 1844.
- [24] A. Berkó, A. Magoni, J. Szökő, *Langmuir* 21 (2005) 4562.
- [25] G.S. Herman, C.H.F. Peden, *Colloids Surf. A* 154 (1999) 187.
- [26] M.A. Henderson, *Surf. Sci.* 419 (1999) 174.